Electrochemical and Solid-State Letters, **12** (9) B126-B130 (2009)
1099-0062/2009/12(9)/B126/5/$25.00 © The Electrochemical Society

In Situ Measurement of Temperature Distribution across a Proton Exchange Membrane Fuel Cell

Sang-Kun Lee, Kohei Ito,[z] Toshihiro Ohshima, Shiun Noda, and Kazunari Sasaki[*]

Department of Mechanical Engineering Science, Kyushu University, Fukuoka 819-0395, Japan

The temperature distribution across a proton exchange membrane fuel cell was measured by inserting micro-thermocouples between layers such as a gas diffusion layer and membrane electrode assembly. Under steady-state operation, the cathode catalyst layer had the maximum temperature. The activation overpotential at the cathode catalyst layer served as the main heat source, resulting in the maximum temperature at the cathode catalyst layer. The temperature at the cathode catalyst layer just after the load current was interrupted had the minimum temperature. This is thought to be caused by water evaporation from the cathode catalyst layer, where liquid water accumulates during operation.
 [DOI: 10.1149/1.3152331]

Manuscript submitted August 25, 2008; revised manuscript received April 20, 2009. Published June 16, 2009.

Water management is a critical issue to obtain a higher performance and longer durability of proton exchange membrane fuel cells (PEMFCs). The temperature distribution and its time evolution in the cell provide key information to establish proper water management because temperature has a large influence on many physical properties in the cell. For instance, temperature determines the water content in polymer electrolyte membrane (PEM), and a slight temperature variation in changes the saturation ratio in cell because of the exponential temperature dependence of water vapor pressure.[1]

Of the three spatial directions for the temperature distribution in the cell, the through-plane direction is especially significant. Mass and heat transport in a cell progress primarily in the through-plane direction, resulting in the development of a temperature distribution in the through-plane direction. Thus, measurement of the temperature across a cell is a key issue for PEMFC research and development.

There are several examples of temperature measurement in PEMFC research. He et al. thinned a thermal sensor and inserted it between two sheets of PEM and measured the temperature in the PEM.[2] Wilkinson et al. embedded several micro-thermocouples at different positions in a flow channel for measurement of the temperature distribution.[3] Hakenjos et al.[4] and Wang et al.[5] measured the temperature distribution using an IR imaging method with focus on the surface of the membrane electrode assembly (MEA). These measurements have contributed to the analysis of thermal behavior in PEMFC; however, they are categorized as measurement for a local point or in an in-plane direction.

The first measurement of temperature distribution in the through-plane direction was reported by Vie and Kjelstrup.[6] They placed four sets of micro-thermocouples in an array and measured the temperature distribution in the through-plane direction. The distribution showed that the temperature at the anode catalyst layer was higher than that at the cathode catalyst layer; they suggested that there was an uncertainty in the measurement and that the obtained temperature was smaller than expected. Thus, the experimental data obtained for the temperature distribution in the through-plane direction have not reached the level to compare with theoretical analysis.

In this study, the temperature distribution in the through-plane direction is shown using micro-thermocouples. Seven thermocouples were inserted between layers as an array across a cell. The temperature distribution in the through-plane direction was successfully obtained without degradation of cell performance. Our method is similar to the work by Vie and Kjelstrup, as mentioned above. We, however, calibrated the thermocouples with close attention and tried to measure the PEM and gas diffusion layer (GDL) temperatures that were not obtained in the previous work, resulting in a more comprehensive measurement for temperature distribution in the through-plane direction. In the following, the placement of the thermocouples in the cell is illustrated, and the temperature distribution obtained during steady-state operation and just after interrupting the load current is discussed.

Experimental

Figure 1 shows a schematic cross section of the cell. To measure the temperature distribution, seven thermocouples were placed across the cell. All the thermocouples were placed in an array; the thermocouple tips were placed in a straight line that ran perpendicular to the plane of the cell. The tips were shifted from this line within 1 mm during the experiment. Three thermocouples were placed on the cathode side: One between the separator and the GDL, the second between two sheets of GDL, and the third between the GDL and the MEA, as shown in Fig. 1. On the anode side, three thermocouples were also placed in the same manner. One thermocouple was placed in the MEA.

To determine whether the insertion of the thermocouples might give an additional electric contact resistance, we measured the *I-V* polarization curve and IR resistance and figured out that the impact of the thermocouple on the contact resistance was practically negligible. The evaluation of the contact resistance is discussed later.

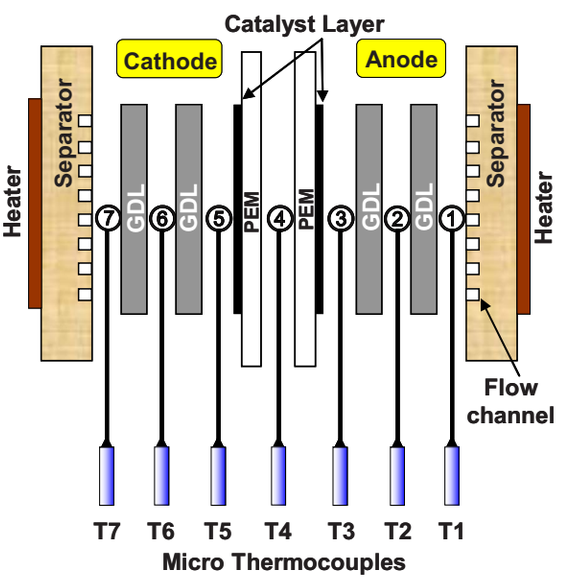

Figure 1. (Color online) Schematic cross section of the cell. Seven micro-thermocouples were placed in an array. The catalyst layer area was 9 cm^2, and the flow channel fabricated on the separator had a serpentine pattern.

* Electrochemical Society Active Member.
[z] E-mail: kohei@mech.kyushu-u.ac.jp

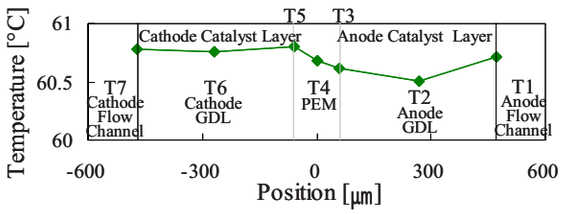

Figure 2. (Color online) Reference temperature obtained when separators' temperatures were controlled at 60°C without load current and gas supply.

The insertion of one thermocouple in the MEA was accomplished in the following manner. Two sheets of MEA were prepared, where the catalyst layer (Pt loading of 1.0 mg/cm^2) was formed on only one side of the PEM (Nafion 112). A thermocouple was then placed between the two fabricated MEA sheets, and they were pressed into one sheet under optimized conditions of 80 N/cm^2 at 132°C for 190 s.

All the thermocouples used were micro-thermocouples (Okazaki, K-type), with a small diameter of 150 μm to minimize the influence of the thermocouples on the electrical, mass, and heat transport in the cell. The thermocouples used here were sheathed type and were electrically insulated so that they could work as the temperature measurement probe in the cell. All the thermocouples were carefully calibrated to give them a high precision. The thermoelectromotive force in the range from 20 to 80°C, corresponding to experimental condition, was measured with a thermostatic chamber, and the calibration curve of each thermocouple was obtained. We measured the temperature in the thermostatic chamber by using the calibrated thermocouple and the calibration curve. This preliminary test gave the thermocouples the precision of ±0.1°C.

Carbon-paper-type (thickness of 200 μm) GDLs were used. Two sheets of GDL were used on both the anode and the cathode side for measurement of the GDL temperature, as shown in Fig. 1. The use of plural sheets of GDL, which was compressible, helped absorb the volume of the thermocouple. The separators had three parallel channel serpentine flow fields for both the cathode and anode. The channel width and height were 1 and 0.5 mm, respectively. The separators were made of stainless steel (SUS316) with gold plating, and a conventional sheath thermocouple was placed in each separator. A sheet-type heater was attached on the back side of each separator. During cell operation, the separator was controlled at a constant temperature using the heater and the sheath thermocouple, resulting in a constant temperature boundary within the precision of ±0.2°C and the response of approximately 100 s.

The reference temperature for each micro-thermocouple was obtained in the following manner. The separator temperature was controlled at 60°C without load current and gas supply, and this state was maintained for 1 h. Although all the micro-thermocouples in the cell should show the same temperature as the separator (60°C), each thermocouple showed a slightly different temperature, as shown in Fig. 2. These temperatures were regarded as the reference temperature for the measurements. The temperatures shown in the next section were denoted as the temperature difference between the measured and the reference temperatures.

In addition to the temperature distribution, IR drop and overpotential were measured using the current-interruption method. The principle of this method was based on the IR-drop characteristic. The response of the IR drop to a sudden change in load current was fast. The response of the activation and concentration overpotential was comparatively slow because these components were located parallel to the electric double-layer capacitance and were influenced by gas diffusion. These features enabled us to separate the IR drop from the overpotentials by interrupting the load current intermittently, namely, by the current-interruption method. The backpressure

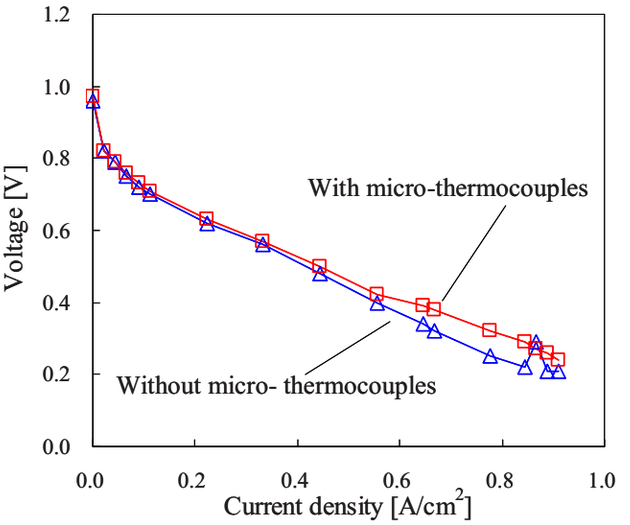

Figure 3. (Color online) *I-V* polarization curves of the cell with/without micro-thermocouples under the following conditions: Cell temperature of 80°C, hydrogen and air flow rate corresponding to a utilization ratio of 0.4 at 1.0 A/cm^2, and an RH of 80%.

of the cell was atmospheric pressure, and the cell was placed in an experimental room within an ambient temperature of approximately 21°C.

Results and Discussion

Influence of thermocouple.— Figure 3 shows *I-V* polarization curves for the cell with and without micro-thermocouples. The MEA of the cell without micro-thermocouples was fabricated in the same way as the MEA of the cell with the micro-thermocouples. The MEA of the cell without micro-thermocouples also consisted of two sheets of PEM. Both of the cells were operated under the conventional condition set: The temperature of the separators was controlled at 80°C, hydrogen gas and air were supplied at a constant flow rate corresponding to a utilization ratio of 0.4 at 1.0 A/cm^2 (stoichiometry of 2.5), and the relative humidity (RH) of the gases was controlled at 80%.

Figure 3 shows that the *I-V* polarization curves of both cells are almost the same. In particular, the *I-V* polarizations agree from 0 to 0.5 A/cm^2. Above 0.5 A/cm^2, the cell with the micro-thermocouples shows a somewhat higher voltage than the cell without the micro-thermocouples. The contact resistance obtained with the current-interruption method, which was done parallel to the measurement of the *I-V* polarization curve, did not show the difference between the cell with and without thermocouples.

The insertion of thermocouples might have an influence on the transport in the cell. The thermocouple blocks the mass, electrical, and heat transport in the through-plane direction in the cell, and the influence of the thermocouple might start to appear in the low current region, resulting in the decrease in cell voltage. However, the cross section of the thermocouple to the through-plane direction is only 1% against the whole electrode area of the cell. The influence of the transport in the through-plane direction can be negligible. Thus, the good agreement appeared in the low current under 0.5 A/cm^2.

The cross section of the thermocouple to the in-plane direction is large; the thermocouple is thought to block the gas transport, liquid water drainage, resulting in the decrease in cell voltage. Beyond this expectation, the cell voltage with thermocouples was 10% higher than that without thermocouples. A possible explanation is that inserting the micro-thermocouple caused the wick effect known as the principle of heat pipe, and that the wick effect promoted the drainage of liquid water in the cell and increased the cell voltage.

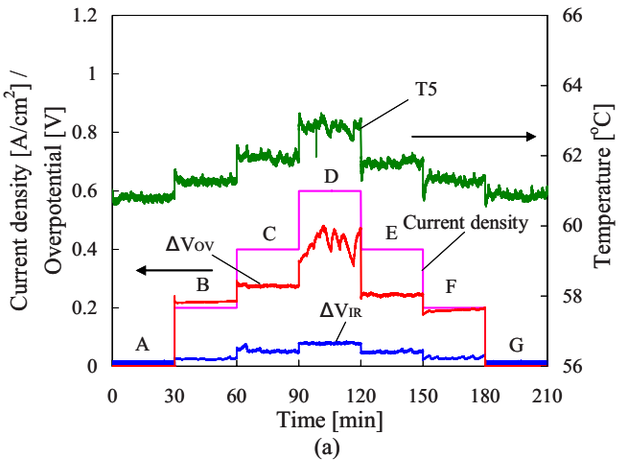

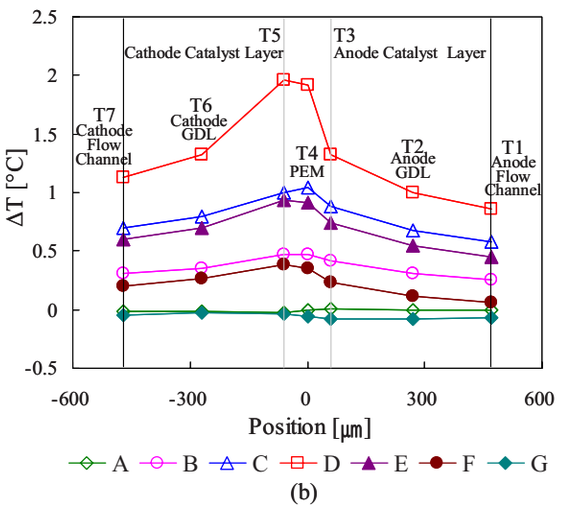

Figure 4. (Color online) Temperature change with changing load current under the following conditions: Separator temperature of 60°C, hydrogen and air flow rate corresponding to a utilization ratio of 0.4 at 1.0 A/cm^2, and an RH of 80%. (a) Time series of temperatures at the cathode catalyst layer and overpotentials. (b) Temperature distributions across the cell for each current density.

Temperature distribution across the cell for various current densities.— Temperature distribution measurements were performed under the following condition set. The separator temperature was maintained at 60°C. Hydrogen gas and air (RH 80%) were supplied at a constant flow rate where the utilization ratio was 0.4 at 1.0 A/cm^2. Under this operation condition set, the open-circuit voltage was 0.97 V. The load current was increased stepwise from 0.0 to 0.6 A/cm^2, and then decreased from 0.6 to 0.0 A/cm^2. Every current regulated was maintained for 30 min.

Figure 4a shows the temperature change with change in the load current. The cathode catalyst temperature, which was measured by the micro-thermocouple placed between the cathode GDL and MEA, is plotted as a representative temperature. IR drop (ΔV_{IR}) and overpotential (ΔV_{OV}) by the current-interruption method are also plotted. Although the overpotential includes both the anode and cathode components, it is thought to practically consist of mainly the cathode component under the present operation.

The loss in electricity generation by PEMFC increases with increasing load current. IR drop and overpotential increased with increasing load current, resulting in increased heat and cathode temperature. During the period of 0.6 A/cm^2, especially in the latter half, the overpotential displayed significant fluctuation, and the cathode temperature also fluctuated according to this fluctuation in the overpotential.

The fluctuation in the overpotential during the period of 0.6 A/cm^2 might be caused by liquid water dynamics. The water produced at the cathode catalyst layer passes through the GDL to the channel, and then drains away from the cell. In this process, water droplets form, each droplet combines, and then the large droplet drains in a burst. This successive water dynamics emerges in a somewhat random fashion and has a significant influence on overpotential. Therefore, the fluctuation in the overpotential is thought to be caused by the water dynamics.

Figure 4b shows the temperature distribution obtained across the cell. The symbols A–G correspond to the current-density condition shown in Fig. 4a. The symbols T1–T7 indicate the positions of micro-thermocouples, as shown in Fig. 1. The temperatures plotted in this figure were obtained from mean time processing for each current-density period.

The highest temperature appeared at the cathode catalyst layer for almost all current conditions. The second highest temperature appeared in the PEM. This temperature distribution is thought to be reasonable with respect to the general PEMFC characteristic, that is, the overpotential at the cathode and the IR drop in the PEM provide the largest and second largest heat sources, respectively. Overall, the temperature distribution measurements using micro-thermocouples captured the general characteristics of PEMFC.

Looking at Fig. 4b closely, there were cases where the temperature at the cathode catalyst was not the highest. For B and C, the temperature in PEM was the highest. In these cases where the load current was in the sequence of a stepwise increase, the wetness in PEM was thought to be relatively poor, leading to a larger IR resistance in PEM compared to the case where the current was in the sequence of a stepwise decrease. Thus, the PEM showed the highest temperature for B and C.

In addition to the IR drop and the overpotential that are categorized in the irreversible heat source, a reversible heat source exists in the cell. The reversible heat source is produced by the entropy change in the half-cell reaction. The amounts of entropy change in the cathode and anode are 0.104 kJ/mol ($H_2 \rightarrow 2H + 2e^-$) and −163.2 kJ/mol ($1/2O_2 + 2H + 2e^- \rightarrow H_2O$), respectively.[7] Converting this entropy change to the 0.6 A/cm^2 equivalent, the reversible heat in the anode is 9.63×10^{-5} W/cm^2 (endothermic). The reversible heat in the cathode is −0.151 W/cm^2 (exothermic). The reversible heat in the anode is negligible than that in the cathode.

The irreversible heat by the overpotential and by the IR drop can be estimated from Fig. 4 under the same current of 0.6 A/cm^2. The overpotential is 0.4 V and corresponds to the irreversible heat of −0.24 W/cm^2 (exothermic). In the same manner, the IR drop is 0.08 V, corresponding to −0.05 W/cm^2 (exothermic). The overpotential comes mainly from the cathode side.

Summing up, the irreversible heat by the overpotential in the cathode is largest, the reversible heat in the cathode is second, and the irreversible heat by the IR drop is third. These heat sources have a main role to form the temperature distribution in the cell.

Transient response of temperature distribution to start-up and shutdown of load current.— This measurement was performed using the following procedure. The supplied gas and the separator temperature were controlled under the same condition as that for the steady-state experiment. The cell was maintained in the state without load current until the cell voltage and temperatures became steady state. The load current was then changed stepwise from 0 to 0.5 A/cm^2. After 1 h, the load current was immediately stopped. During these operations, the temperatures, IR drop, and overpotential were continuously measured.

Figure 5a shows the temperature variations at the anode flow channel (T1), the anode catalyst layer (T3), and the cathode catalyst layer (T5) when the load current was changed stepwise from 0 to

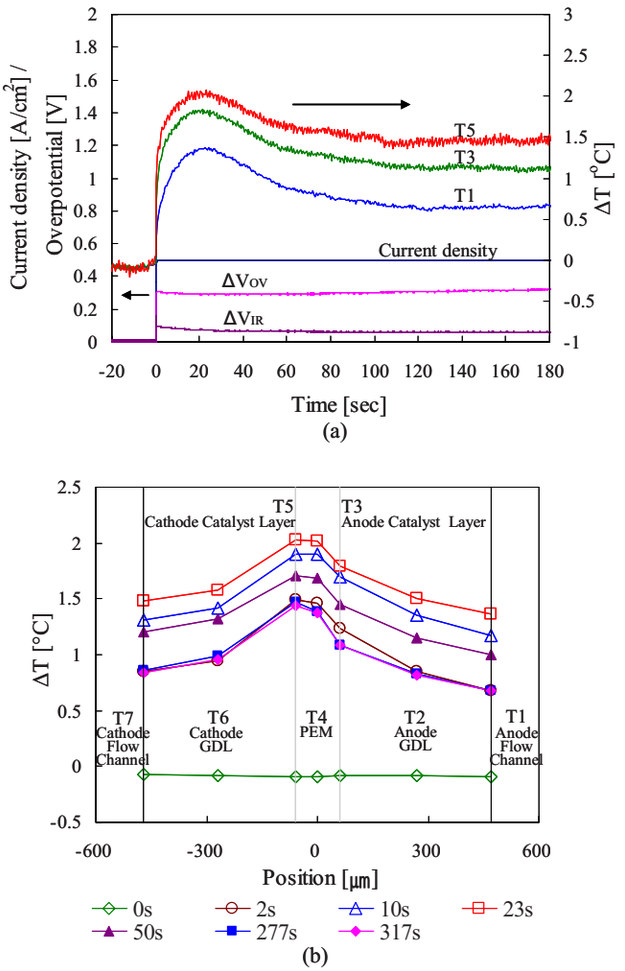

Figure 5. (Color online) (a) Temperature variations at the anode flow channel (T1), the anode catalyst layer (T3), and the cathode catalyst layer (T5) when the load current was changed stepwise from 0 to 0.5 A/cm^2. (b) Temperature distributions across the cell after the load current was applied.

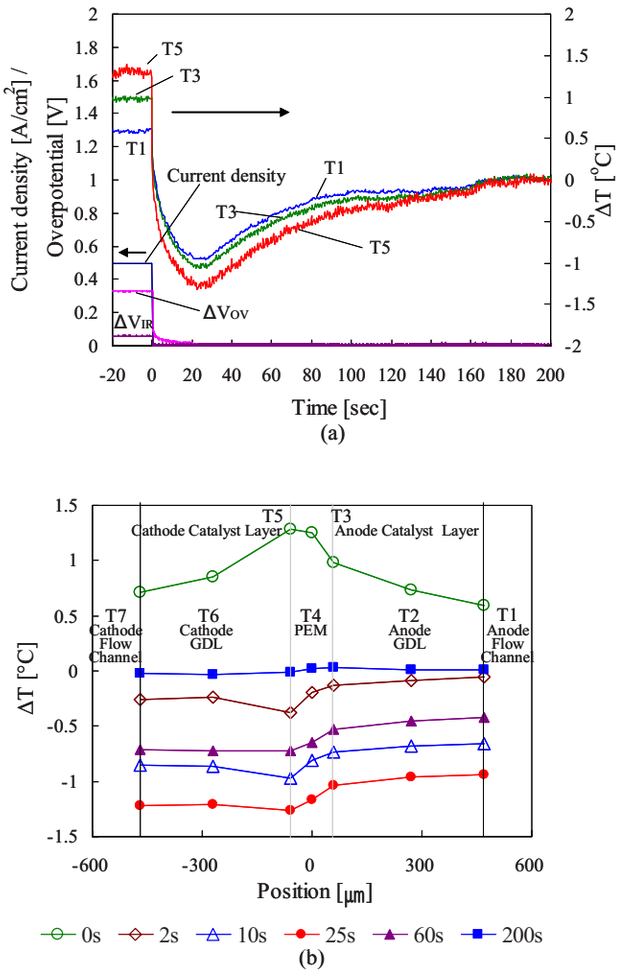

Figure 6. (Color online) (a) Temperature variations at the anode flow channel (T1), the anode catalyst layer (T3), and the cathode catalyst layer (T5) when the load current was changed stepwise from 0.5 to 0 A/cm^2. (b) Temperature distributions across the cell after the load current was stopped.

0.5 A/cm^2. The IR drop and overpotential are also shown. These losses, which function as a heat source, increased stepwise corresponding to the change in the load current.

All the temperatures observed increased slowly compared to the change in the IR drop and overpotential. After 23 s, the increase in the temperatures began to decrease and then stabilized, exhibiting an overshoot profile.

Among the three temperatures (T1, T3, and T5), the cathode catalyst layer had the maximum temperature after the current was applied. The anode catalyst and the anode flow channel had the second and the third highest temperatures, respectively. The overpotential at the cathode catalyst layer performed as the main heat source, and the heat was conducted to each layer in the through-plane direction, causing the temperature difference between the layers.

The overshoot of the temperature was caused by the time delay of a temperature controller built into the separators. The exotherm started just after the current was applied, and it heated the separator in addition to the interior of the cell, resulting in the increased temperature of the separators. Due to the large heat capacitance of the separators, the temperature controller began to work after a while, resulting in reducing the temperature of the separators slowly. This time delay can be estimated from the simple modeling based on the unsteady heat conduction equation with the thermal properties of the separator (SUS316)

$$\tau_{\text{separator}}^{\text{heat}} = \frac{\rho_{\text{SUS}} c_{\text{P,SUS}} L_{\text{separator}}^2}{k_{\text{SUS}}}$$

$$= \frac{7.98 \times 10^3 \text{ kg m}^{-3} \times 502 \text{ J kg}^{-1} \text{ K}^{-1} \times (0.02 \text{ m})^2}{16.3 \text{ W m}^{-1} \text{ K}^{-1}}$$

$$= 98 \text{ s}$$

ρ_{SUS}, $c_{\text{P,SUS}}$, $L_{\text{separator}}$, and k_{SUS} are the density, heat capacity, thickness, and thermal conductivity, respectively. The time delay of the heat conduction in the separator roughly agrees with the time scale of the overshoot in Fig. 5a. Thus, the temperatures of T5, T3, and T1 displayed an overshoot as they were synchronized with the separator temperature.

Figure 5b shows the temperature distributions across the cell at selected times. Overall, the temperature at the cathode side was higher than that at the anode side, and the cathode catalyst layer had the maximum temperature. This also suggests that the overpotential at the cathode catalyst layer is the largest heat source across the cell.

Figure 6a shows the variation in temperature, IR drop, and overpotential when the load current was stopped. The IR drop decreased in a stepwise fashion, synchronizing with the current change. However, the overpotential decreased slowly compared to the IR drop.

After the current was interrupted, the heat source due to the IR drop and overpotential disappeared, and each temperature of the T1,

T3, and T5 decreased. After 30 s, the temperatures began to increase as the temperature controller began to work, and then all the temperatures converged to 60°C. These temperature variations can be regarded as practical temperature behavior when the load current is interrupted under constant cell-temperature operation.

The cathode catalyst temperature of T5 displayed the minimum temperature after the current was stopped, although it was previously the maximum temperature. The anode flow channel temperature of T3 had the maximum temperature after the current was interrupted, although it was previously the minimum temperature. These features are also confirmed in Fig. 6b.

A possible explanation for the minimum temperature at the cathode catalyst layer is in the following. During cell operation, water is produced at the cathode catalyst layer and partially condenses there as liquid water. The liquid water is drained away through the cathode flow channel. Accordingly, the liquid water spreads in the cathode side with the maximum content at the cathode catalyst layer. After the current is stopped, evaporation of the liquid water at the cathode side progresses because air, which is not saturated, is continuously supplied. Then the latent heat for the evaporation of liquid water cools the cathode catalyst layer. The latent heat for the PEM water desorption[8] is a candidate to cool the catalyst layer. Hence, the cathode catalyst layer had the minimum temperature after the current was stopped.

The overpotential time delay of 20 s, after the load current was interrupted, is evaluated here with the oxygen diffusion in GDL. The oxygen gas is redistributed in GDL when the current is interrupted, and this redistribution changes the overpotential. Based on this modeling, the time delay can be estimated from the square of the GDL thickness divided by an equivalent diffusion coefficient

$$\tau_{\mathrm{GDL}}^{\mathrm{diffusion}} = \frac{(2L_{\mathrm{GDL}})^2}{\varepsilon D_{\mathrm{N_2\text{-}O_2}}} = \frac{(2 \times 0.0002\ \mathrm{m})^2}{0.21 \times 3.18 \times 10^{-5}\ \mathrm{m^2\ s^{-1}}} = 0.024\ \mathrm{s}$$

ε, L_{GDL}, and $D_{\mathrm{N_2\text{-}O_2}}$ are the GDL porosity, GDL thickness, and relative diffusion coefficient between nitrogen and oxygen, respectively. The time delay estimated from the oxygen diffusion is 24 ms, which is much shorter than that of the overpotential. The oxygen diffusion did not cause the time delay of the overpotential in Fig. 6a.

Conclusion

The temperature distribution in the through-plane direction in a PEMFC was obtained and evaluated by insertion of micro-thermocouples under the conventional operating condition. Under steady-state operation, the cathode catalyst layer had the maximum temperature corresponding to the cathode overpotential, which functioned as the main heat source. The cathode catalyst layer had the minimum temperature just after the load current was stopped. Latent heat for water evaporation on the cathode catalyst layer, where liquid water accumulated during operation, was suggested as the cause for the minimum temperature at the cathode catalyst layer. Temperature distribution measurement by insertion of micro-thermocouples did not have a large influence on the cell performance. The temperature measurement method introduced in this study will contribute to the development of PEMFCs, especially in the area of water management.

Kyushu University assisted in meeting the publication costs of this article.

References

1. Y. A. Çengel and M. A. Boles, *Thermodynamics: An Engineering Approach*, 6th ed., McGraw-Hill, New York (2008).
2. S. He, M. M. Mench, and S. Tadigadapa, *Sens. Actuators, A*, **125**, 170 (2006).
3. M. Wilkinson, M. Blanco, E. Gu, J. J. Martin, D. P. Wilkinson, J. J. Zhang, and H. Wang, *Electrochem. Solid-State Lett.*, **9**, A507 (2006).
4. A. Hakenjos, H. Muenter, U. Wittstadt, and C. Hebling, *J. Power Sources*, **131**, 213 (2004).
5. M. Wang, H. Guo, and C. Ma, *J. Power Sources*, **157**, 181 (2006).
6. P. J. S. Vie and S. Kjelstrup, *Electrochim. Acta*, **49**, 1069 (2004).
7. M. J. Lampinen and M. Famina, *J. Electrochem. Soc.*, **140**, 3537 (1993).
8. T. Watari, H. Wang, K. Kuwahara, K. Tanaka, H. Kita, and O. Ken-ichi, *J. Membr. Sci.*, **219**, 137 (2003).